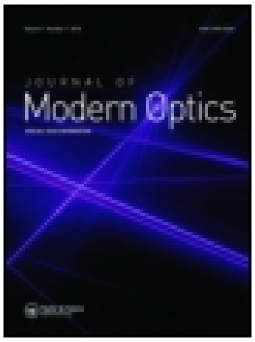

Taylor & Francis
Taylor & Francis Group

Journal of Modern Optics

ISSN: (Print) (Online) Journal homepage: https://www.tandfonline.com/loi/tmop20

Multi-wavelength switchable random fibre laser based on double Sagnac-loop filter

Honggang Pan, Taotao Guo, Ailing Zhang & Chang Liu

JOURNAL OF MODERN OPTICS
https://doi.org/10.1080/09500340.2021.1961906

Multi-wavelength switchable random fibre laser based on double Sagnac-loop filter

Honggang Pan, Taotao Guo, Ailing Zhang and Chang Liu

Engineering Research Center of Optoelectronic Devices & Communication Technology, School of Electrical and Electronic Engineering, Tianjin Key Laboratory of Film Electronic and Communication Devices, Ministry of Education, Tianjin University of Technology, Tianjin, People's Republic of China

ABSTRACT
A multi-wavelength switchable random fibre laser based on a double Sagnac-loop filter is proposed. The threshold of laser is 27 mW and the slope efficiency of the total power output to pump power is about 0.04%. In the experiment, stable and switchable laser outputs of single-, dual-, tri- and quad-wavelength channels are obtained by adjusting the polarization controller at room temperature. The wavelength positions are tuneable within the range of 1556–1564 nm and intervals are switchable between 2.5, 5 and 7.5 nm. Under 300 mW pump power, average power intensity of −24dBm is achieved. Furthermore, the output of fibre laser is relatively stable with less than 0.2 nm wavelength drift and less than 1.5 dBm power fluctuation within one hour. The proposed random fibre laser has promising application prospects for distributed sensing systems and biomedical imaging.

ARTICLE HISTORY
Received 15 May 2021
Accepted 23 July 2021

KEYWORDS
Random distributed feedback; multi-wavelength switchable; double Sagnac-loop filter; Rayleigh scattering; wavelength intervals switchable; random fibre laser

Introduction

In recent years, a new type of random fibre laser that has no need for a conventional fibre laser has attracted wide attention. It uses the inherent or artificial random scattering medium in the fibre as the feedback mechanism of laser formation without the need for a well-defined resonant cavity, making the design of the fibre laser more approachable. Since the concept of the distributed feedback random fibre laser was proposed in 2010 [1], random fibre lasers (RFLs) have made great progress and achieved a series of research results, impacting numerous research fields including optical fibre communication, sensing and imaging [1–3].

Switchable multi-wavelength fibre lasers have attracted attention due to potential applications in dense wavelength division multiplexing (DWDM) optical communication systems [4], fibre sensing [5], microwave signal generation [6], spectroscopy [7], and so on. A typical approach is to use a comb filter to produce a multi-wavelength output, such as tilted fibre grating (TFG) [8], fibre-Bragg-grating (FBG) [9], Sagnac-loop [10], Mach–Zehnder interferometer (MZI) [11], mode interference [12] and Lyot filters[13].

Inspired by conventional multi-wavelength fibre lasers, multi-wavelength random fibre lasers (MWRFL) based on comb filters are proposed. Some researchers have used fibre grating arrays [14,15], all-fibre Lyot filters [16,17], and Sagnac-loop filters [18–21] and MZI [22,23] to produce stable multi-wavelength random fibre lasers. In 2005, S. Sugavanam [17] realized a random distributed feedback multi-wavelength fibre laser by using an all-fibre Lyot filter. The number of lines generated can be as high as 50, but the wavelength interval cannot be changed. In 2019, T. Feng [15] demonstrated experimentally six-wavelength channels random fibre laser using a 2 km-long single-mode fibre together with six-superimposed fibre-Bragg-gratings. However, the number of wavelengths and intervals cannot be changed. In 2020 and 2021, J. W. Liu realized multi-wavelength switchable random fibre lasers based on RDFB using a two-stage Sagnac-loop mirror [21], dual-pass MZI [22] and compound filter (a dual-pass MZI and a Sagnac-loop) [23], respectively. Similarly, the wavelength interval of these MWRFL outputs is constant.

In this paper, a multi-wavelength switchable Erbium-doped random fibre laser is proposed and verified by experiment. The threshold of the laser is 27 mW. Stable and switchable laser output of single-, dual-, tri- and quad-wavelength channels can be obtained by adjusting the PCs of the double Sagnac-loop filter (DSLF). The wavelength position is tuneable, and the wavelength interval can be adjusted between 2.5, 5 and 7.5 nm. Using 300 mW, the average power intensity is about −24 dBm. Furthermore, the wavelength drift within one hour is less

CONTACT Ailing Zhang alzhang@email.tjut.edu.cn

than 0.2 nm, and the power fluctuation is less than 1.5 dBm. Compared to existing fibre lasers, the DSLF has the advantages of simple fabrication, low laser threshold value and stability.

Experimental setup and principles

The experimental setup is shown in Figure 1. A 980 nm pump source (VLSS-980-B) with a 350 mW maximum power output is used to pump the EDF through a 980/1550 nm wavelength division multiplexer (WDM). The gain medium is a 10 m-long EDF (EDFC-980-HP, Nufern), whose core and cladding diameter is 6 and 125 μm, respectively. The other end of the EDF was connected to a DSLF, which is a tuneable multi-wavelength filter. The filter consisted of three 3 dB couplers, OC1, OC2 and OC3, two polarization-maintaining fibres (PMF) with different lengths, PMF1 and PMF2, and two polarization controllers, PC1 and PC2. The DSLF is also used as a mirror to form a half-open cavity structure. The 1550 nm port of the WDM is connected to the 25 km-long SMF (SMF-28) which provides RDFB through back Rayleigh scattering (RS). An isolator (ISO) prevents Fresnel reflection and ensuring that the feedback is all caused by the RS. The obtained spectra are collected by the optical spectrum analyser (OSA, YOKOGAWA-70D) with a resolution of 0.02 nm. An optical power meter (PMSII-A) is connected to the end of SMF to measure the total power output of the MWRFL. All experiments in this work are carried out at room temperature (25°C).

The schematic diagram of the proposed DSLF is shown in Figure 2. As designed, when the incident light enters the 3 dB coupler OC1 from port 1, it is divided into two beams, where one travels clockwise (forward) through port 3, and the other beam travels counter-clockwise (reverse) through port 4, and then return to the coupler coherent output through two PCs and PMFs, respectively. The light fields of ports 1, 2, 3 and 4 are assigned as $E_1.E_2, E_3$ and E_4, respectively. E_3 and E_4 are divided into two equal beams (E_5 and E_6, E_7 and E_8) by the 3 dB couplers OC2 and OC3, respectively. After a circle of light transmission in a DSLF, the transmittance calculated as [10]:

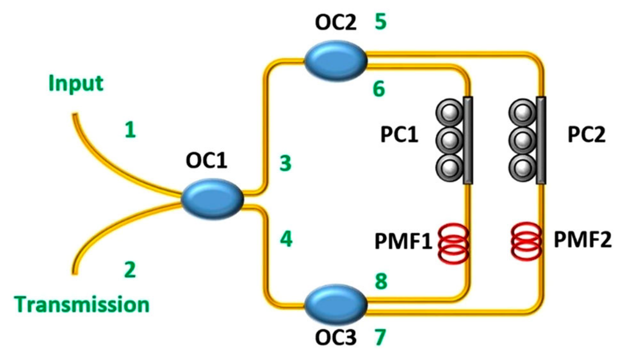

Figure 2. Schematic diagram of DSLF filter.

$$T = \frac{1}{4}(1 + \cos\theta_1 \cos\theta_2 \sin(\varphi_2 - \varphi_1) - \sin\theta_2^2 \cos\varphi_2 \sin\varphi_2 + \sin\theta_1^2 \cos\varphi_1 \sin\varphi_1)$$

where θ_1 and θ_2 are the polarization angles of the light passing PC1 and PC2, respectively. $\varphi = \pi \Delta nL/\lambda$ is the phase difference caused by polarization mode dispersion when the light travels on the fast and slow axes. L is the length of PMF and Δn is the effective refractive index difference between the fast and slow axes. λ is the wavelength of light.

In this experiment, the lengths of PMF1 and PMF2 are 0.5 m and 2 m, respectively. When $\theta_1 = \pi/3$, $\theta_1 = \pi/6$ and $\theta_1 = 0$, $\theta_1 = \pi/4$, the simulated transmission spectra are shown in Figure 3(a–d) depicts two typical modes of all output comb transmission spectra of a DSLF at different PC angles. From Figure 3, the filter can realize wavelength switching, and the wavelength interval is an integral multiple of 2.5 nm.

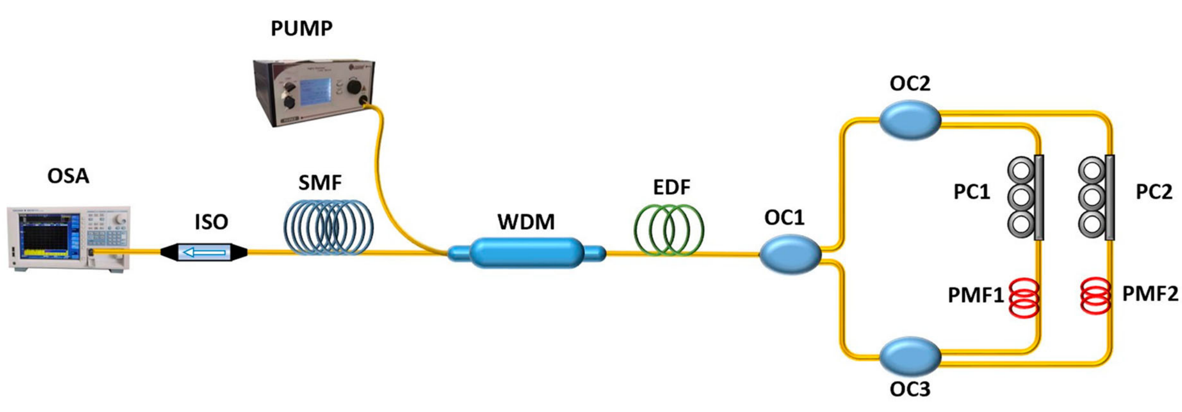

Figure 1. Experimental setup diagram of a multi-wavelength switchable random fibre laser.

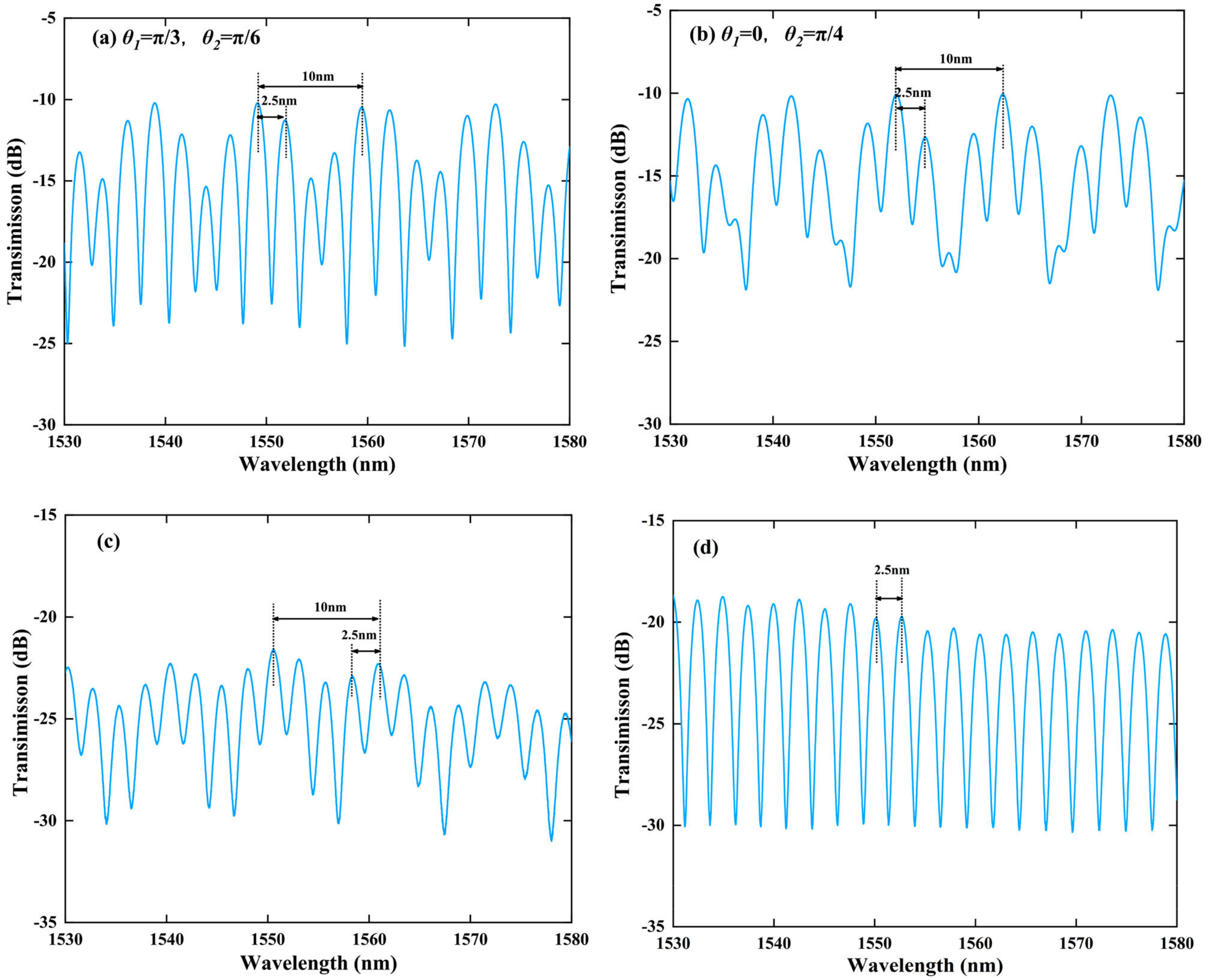

Figure 3. Transmission spectra of the DSLF filter. (a) Simulated transmission spectra of $\theta_1 = \pi/3, \theta_1 = \pi/6$. (b) Simulated transmission spectra of $\theta_1 = 0, \theta_1 = \pi/4$. (c) and (d) are the measured transmission spectra.

Experimental results and analysis

When the pump power is slightly above the threshold value of 27 mW, in Figure 4(a), the laser output is obtained. Figure 4(b–f) show the laser spectra measured under the pump power of 50, 160, 220, 250 and 300 mW, respectively. When the pump power is 50 mW, only one laser channel appeared. As the pump power increases, the number of channels increases from 1 to 4. It can be seen that the linewidths of each laser channel become wider with the increasing pump power. When the pump power reaches 300 mW, the average linewidth of the laser channel is about 0.3 nm and the average power intensity of the laser channel is ~ -25 dBm. Therefore, it can be predicted that more laser channels will be generated as the pump power continues to increase.

In addition, we can see from the illustration of Figure 4 that each channel contains several relatively distinct emission lines or spikes which are separated by an integral multiple of 0.08 nm and are unstable with time as determined by further detailed measurement. Based on References [18,21,24], we speculate that these emission lines are Stokes lines generated by stimulated Brillouin spectroscopy (SBS) in the SMF. These Stokes lines are amplified twice by the EDF through the reflection of the DSLF and then fed into the SMF again. In the SMF, they resonated in the laser cavity by the RDFB of RS. With the increase of pump power, the power of low-order Stokes exceeds the threshold, resulting in high-order SBS lines, so each laser channel has more emission lines. The intensity of random emission lines also increases with the increasing pump power. Therefore, the multi-order SBS emission lines make the random lasing channel wider and stronger. The unstable laser emission (as a common feature of this class of lasers) is mainly caused by the RDFB in the SMF through RS. And each laser channel

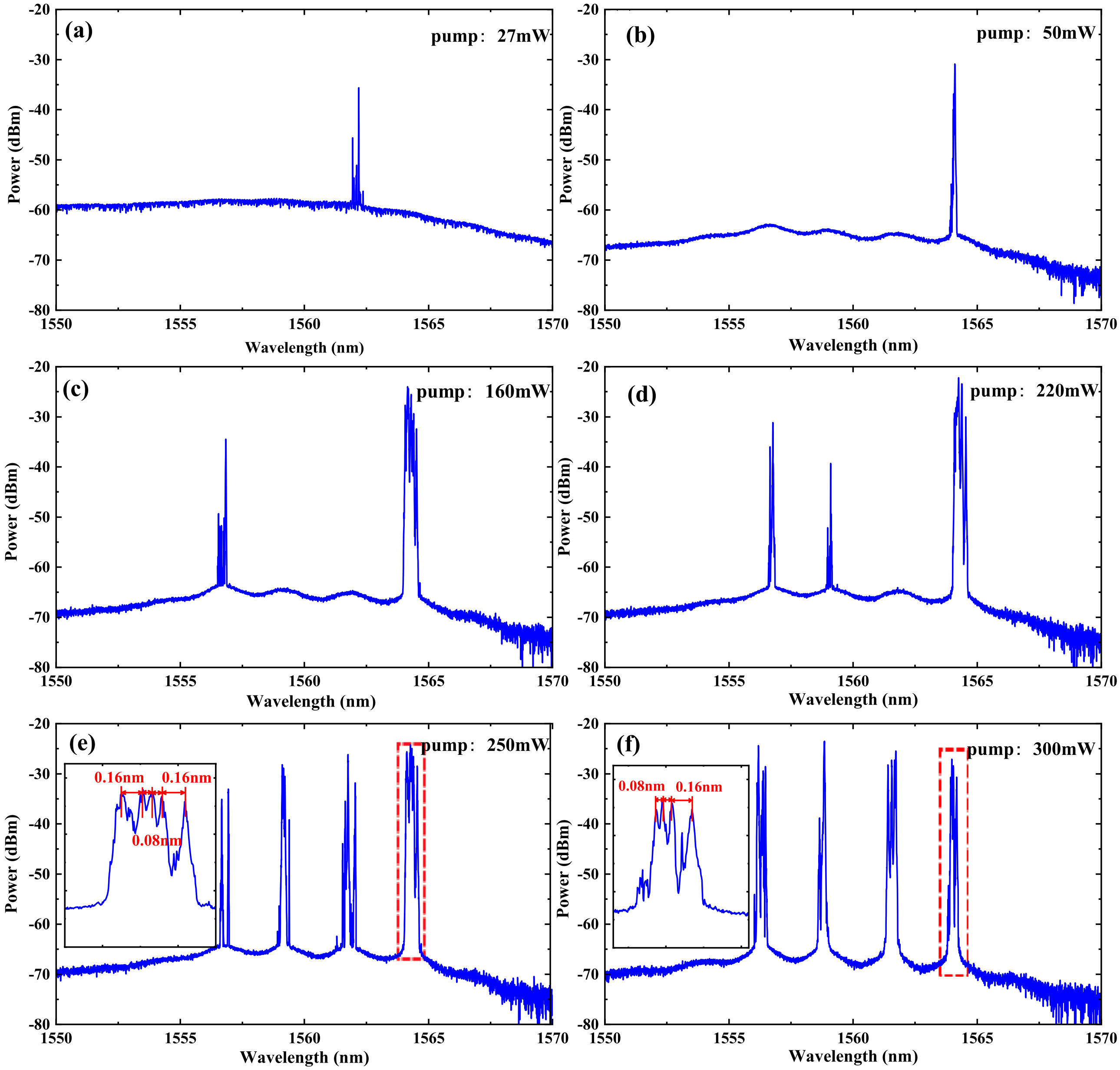

Figure 4. Laser spectra with a pump power of 27, 50, 160, 220, 250 and 300 mW, respectively. The illustrations are amplifying single channel spectra.

has inconspicuous noise. A section of passive erbium-doped fibre or erbium-ytterbium co-doped fibre can be inserted into the cavity to suppress the mode competition in the cavity to eliminate the noise [*25*]. Passively doped fibre can also be added to the output port to reduce the linewidth, and then reduce the noise.

Under the pump power of 300 mW, a stable single channel laser appears by adjusting the two PCs, with the central wavelengths of 1556.3, 1558.8, 15612.3 and 1563.8 nm, respectively, as shown in Figure 5. The power intensity of the laser channel is ~ -21 dBm, and the narrowest linewidth and the widest linewidth are about 0.3 and 0.7 nm, respectively.

Stable dual-wavelength channel lasing is also observed in our work. Wavelength interval tuning can be achieved by carefully adjusting the PCs, as shown in Figure 6. The wavelength interval is the largest at 7.5 nm, Figure 6(h). In addition, we measured the wavelength interval at 2.5 nm (Figure 6(a, c, e, g)) and 5 nm (Figure 6(b, d, f)). In the whole process of adjusting PCs, the wavelength positions are tuning from Figure 6. The intensity of the dual-wavelength channel is ~ -22 dBm, and the power difference between the two wavelengths is less than 1 dBm. In addition, the linewidth of a single channel almost does not change during the tuning process, which is approximately 0.7 nm.

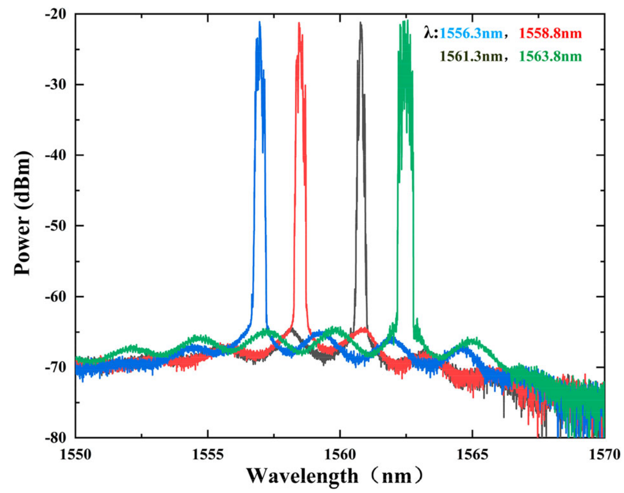

Figure 5. Single-wavelength channel laser output spectra.

During the experiment, the laser output of the tri-wavelength channel is also observed. Tri-wavelength and wavelength interval tuning is achieved by slowly adjusting the PCs, as shown in Figure 7. And the wavelength intervals are 2.5 and 5 nm. The intensity of the three wavelength channels is ∼ −23 dBm, and the intensity difference of the wavelength channel is less than 3 dBm. In addition, the linewidth of each channel is almost unchanged in the tuning process, which is about 0.5 nm, slightly narrower than that of the dual-wavelength channel. This is because the tri-channel output has slightly fewer Stokes lines in each channel than the dual-channel output.

In addition, when the PC is tuned to a certain angle, a stable quad-wavelength channel laser output occurred. As shown in Figure 8, and the wavelength interval is 2.5 nm with a linewidth of ∼0.3 nm and average power intensity of ∼ −25dBm.

To test the stability of the laser output of the quad-wavelength channel, the angle and pump power of the PCs are kept unchanged in the experiment. Figure 9(a) shows the spectra output from scanning every 10 min for an hour. During the experiment, under the 300 mW

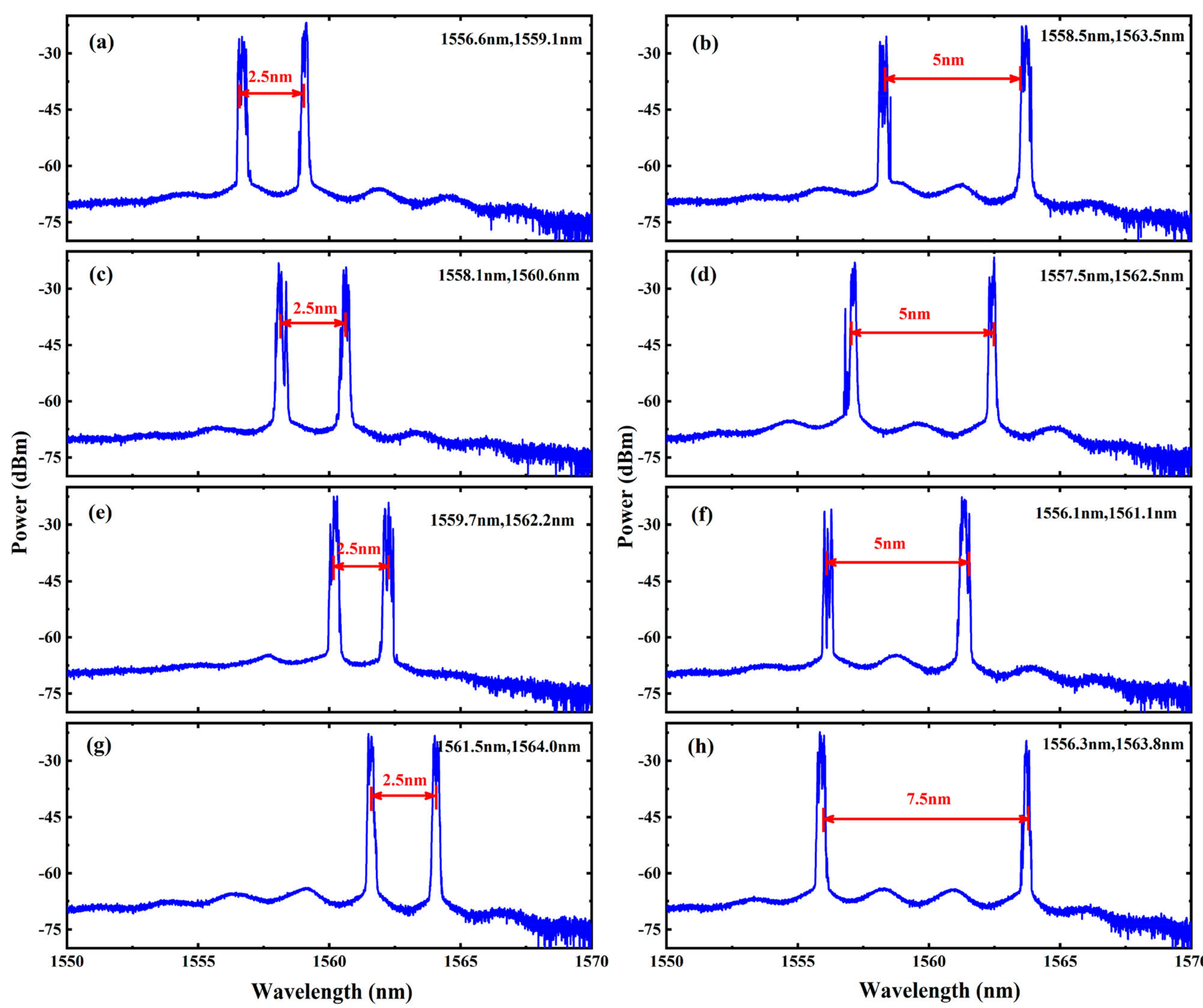

Figure 6. Dual-wavelength channel lasing spectra.

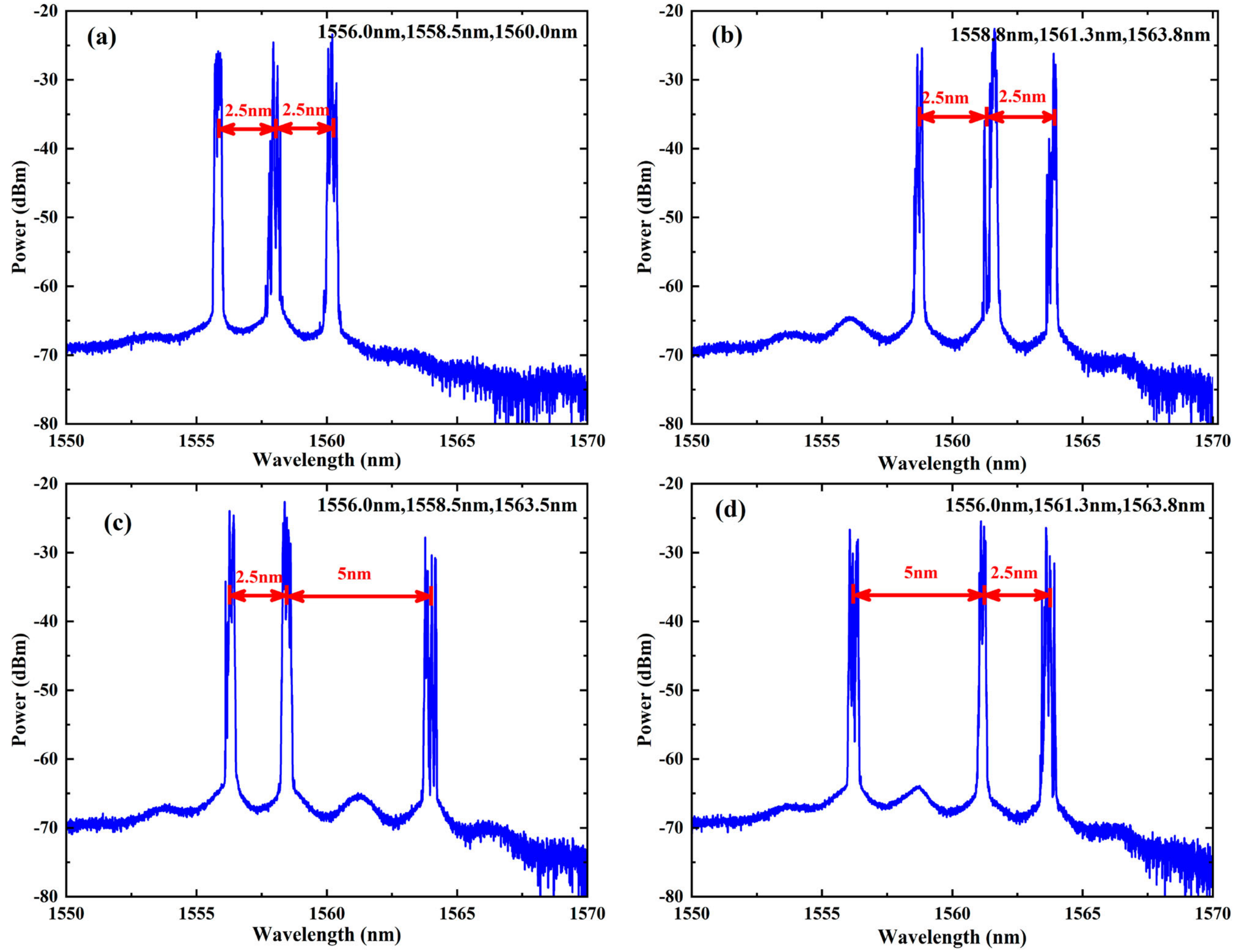

Figure 7. Tri-wavelength channel lasing spectra.

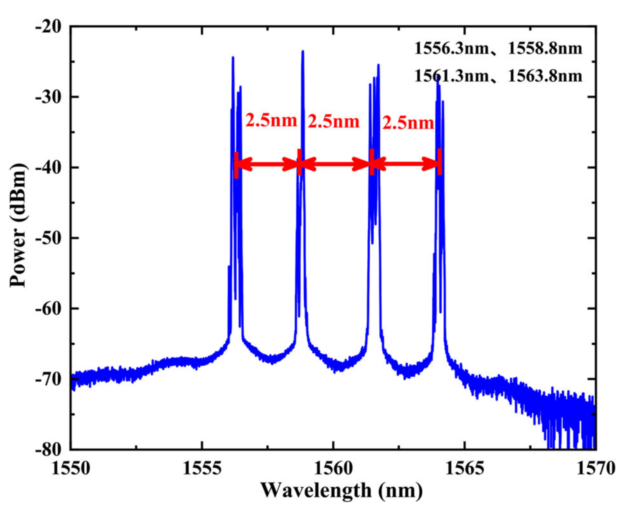

Figure 8. Laser output spectra of the quad-wavelength channel.

pump power, there are four laser channels in the wavelength range of 1556.1–1564.0 nm, and all of the output spectra show constant quad-wavelength channel lasing with the power output of each channel maintain at ∼ −25 dBm. Figure 9(b) shows each wavelength shift (black line) and power fluctuation (red line) of the quad-wavelength channel laser output. The measurement results show that the single central wavelength drift of the quad-wavelength channel laser output within 1 h is less than 0.2 nm and the power fluctuation is less than 1.5 dBm. In addition, we can find that the power of the channel varies greatly on both sides, which may be caused by the mode competition derived from randomly cascaded SBS, distributed RS, and pump EDF. The gain of EDF has a peak at 1560 nm at the pump of 300 mW, so the channel power in the middle is higher than that on the two sides and the multi-order SBS emission lines are more stable, so the power is more stable. Therefore, we conclude that the output of the quad-wavelength channel is relatively stable.

For the laser output, we investigate the relationship between the total power output and the pump power. The measurement result is shown in Figure 10, and the threshold for RFL was 27 mW. When the pump power exceeds the laser threshold, the power output begins to

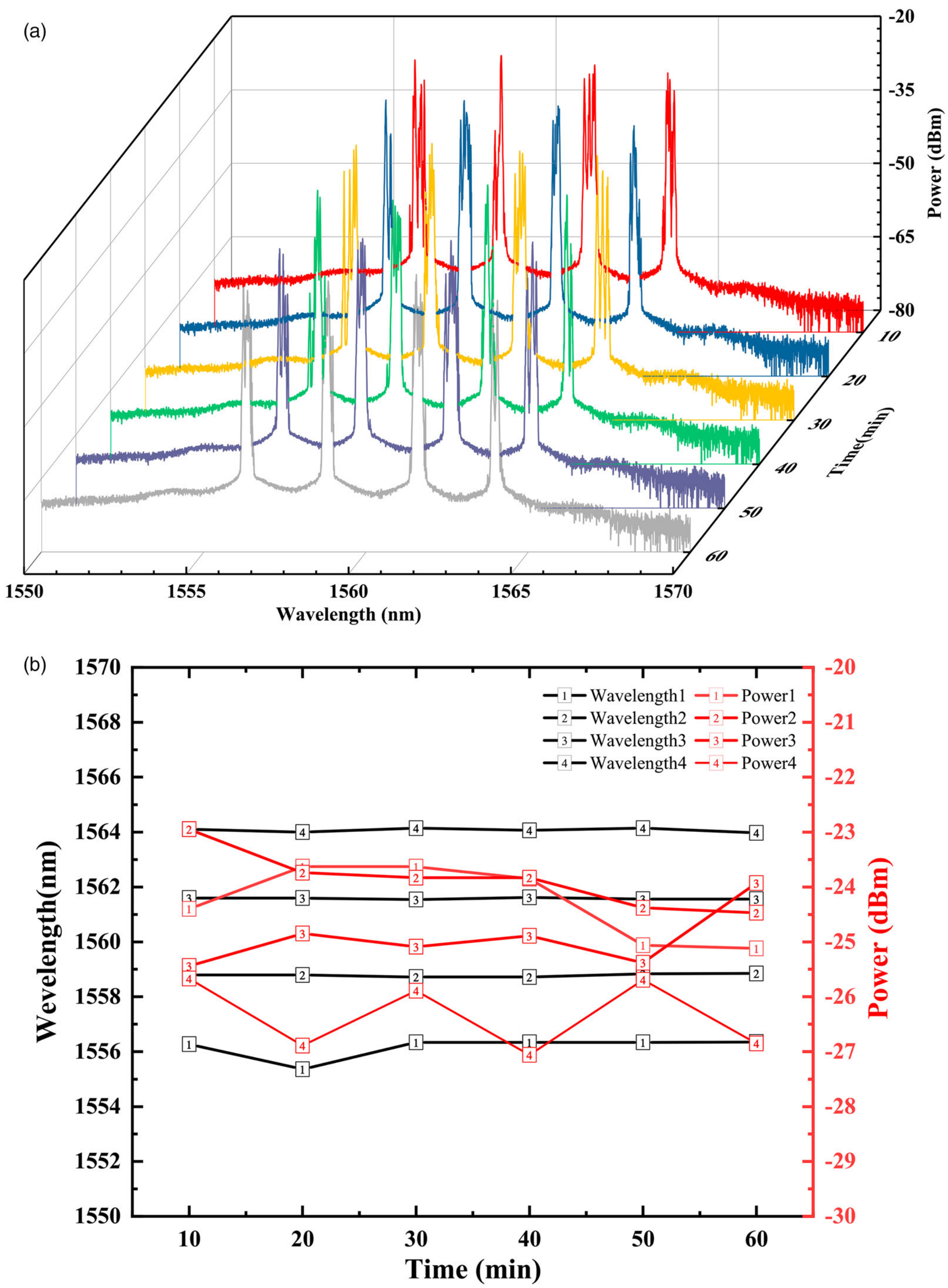

Figure 9. Stability of laser output in the quad-wavelength channel. (a) Repeatedly scans of the output spectra of the four-wavelength channels every 10 min. (b) Outputs the central wavelength (black) and power (red) of each of the four channels every 10 min.

increase linearly, and the fitting slope efficiency is about 0.04%. In addition, the efficiency of the laser can be improved by reducing the total loss of the experimental setup and the length of the SMF.

Conclusion

In conclusion, we have experimentally demonstrated a multi-wavelength switchable erbium-doped random fibre laser with a DSLF comb filter. The threshold of RFL is 27 mW, and the slope efficiency of the total power output to pump power was about 0.04%. When the pump power is 300 mW, single-, dual-, tri- and quad-wavelength tuneable laser outputs are achieved by adjusting the two PCs, and the wavelength interval is tuneable between 2.5, 5 and 7.5 nm. With time, the multi-channel random laser output remained relatively stable. The switchable multi-wavelength random fibre laser has

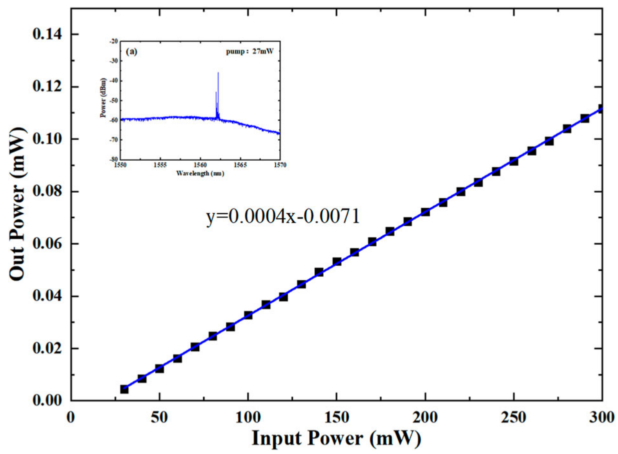

Figure 10. The output laser power is compared with the pump power.

the advantages of a low laser threshold and stable output. And it has potential applications in fields using multi-wavelength lasers, sensing, communication and imaging.

Disclosure statement

No potential conflict of interest was reported by the author(s).

ORCID

Taotao Guo http://orcid.org/0000-0002-1963-2820

References

[1] Turitsyn SK, Babin SA, El-Taher AE, et al. Random distributed feedback fiber laser. Nat Photonics. 2010;4:231–235.
[2] de Matos CJS, Menezes de SL, Brito-Silva AM, et al. Random fiber laser. Phys Rev Lett. 2007;99(15):153903.
[3] Turitsyn SK, Babin SA, Churkin DV, et al. Random distributed feedback fibre lasers. Phys Rep. 2014;542(2):133–193.
[4] Tzeng S-L, Chang H-C, Chen Y-K. Limiting-amplified multiwavelength dispersion compensator incorporating chirped fiber gratings and optical amplifier for DWDM systems. Opt Commun. 1999;169(1–6):81–86.
[5] Wang ZN, Rao YJ, Wu H, et al. Long-distance fiber-optic point-sensing systems based on random fiber lasers. Opt Express. 2012;20(16):17695–17700.
[6] Xiaoying H, Wang DN, Liao CR, et al. Tunable and switchable dual-wavelength single-longitudinal-mode erbium-doped fiber lasers. J Lightwave Technol. 2011;29(6):842–849.
[7] Boussaad S, Pean J, Tao NJ. High-resolution multiwavelength surface plasmon resonance spectroscopy for probing conformational and electronic changes in redox proteins. Anal Chem. 2000;72(1):222–226.
[8] Mou C, Saffari P, Fu H, et al. Single- and dual-wavelength switchable erbium-doped fiber ring laser based on intracavity polarization selective tilted fiber gratings. Appl Optics. 2009;48(18):3455–3459.
[9] Yin B, Feng S, Liu Z, et al. Tunable and switchable dual-wavelength single polarization narrow linewidth SLM erbium-doped fiber laser based on a PM-CMFBG filter. Opt Express. 2014;22(19):22528–22533.
[10] Tang M, Jiang Y, Li H, et al. Multi-wavelength fiber laser based on dual-Sagnac comb filter for LP11 modes output. J Lightwave Technol. 2020;38(14):3745–3750.
[11] Luo A-P, Luo Z-C, Xu W-C, et al. Wavelength switchable flat-top all-fiber comb filter based on a double-loop Mach-Zehnder interferometer. Opt Express. 2010;18(6):6056–6063.
[12] Qi Y, Kang Z, Sun J, et al. Wavelength-switchable fiber laser based on few-mode fiber filter with core-offset structure. Opt Laser Technol. 2016;81:26–32.
[13] Zhao Q, Pei L, Zheng J, et al. Switchable multi-wavelength erbium-doped fiber laser with adjustable wavelength interval. J Lightwave Technol. 2019;37(15):3784–3790.
[14] Xu Y, Liang Z, Liang C, et al. Single-mode SOA-based 1kHz-linewidth dual-wavelength random fiber laser. Opt Express. 2017;25(14):15828–15837.
[15] Feng T, Jiang M, Ren Y, et al. High stability multi-wavelength random erbium-doped fiber laser with a reflecting-filter of six-superimposed fiber-Bragg-gratings. OSA Continuum. 2019;2(9):2526–2538.
[16] Sugavanam S, Yan Z, Kamynin V, et al. Multiwavelength generation in a random distributed feedback fiber laser using an all fiber Lyot filter. Opt Express. 2014;22(3):2839–2844.
[17] Sugavanam S, Zulkifli MZ, Churkin DV. Multi-wavelength erbium/Raman gain based random distributed feedback fiber laser. Laser Phys. 2016;26(1):015101.
[18] Liu Y, Dong X, Jiang M, et al. Multi-wavelength erbium-doped fiber laser based on random distributed feedback. Appl Phys B-Lasers Opt. 2016;122(9):240.
[19] Wu H, Song J, Liu W, et al. High power high signal-to-noise ratio multiwavelength Raman fiber laser based on random distributed feedback. J Appl Phys. 2017;56(11):110304.
[20] Saleh S, Cholan NA, Sulaiman AH, et al. Stable multi-wavelength erbium-doped random fiber laser. IEEE J Sel Top Quantum Electron. 2018;24(3):1–6.
[21] Liu J, Tong Z, Zhang W, et al. Switchable multi-wavelength erbium-doped random distributed feedback fiber laser incorporating two-stage Sagnac filter. Laser Phys. 2020;30(11):115101.
[22] Liu J, Tong Z, Zhang W, et al. Tunable multi-wavelength random distributed feedback fiber laser based on dual-pass MZI. Appl Phys B-Lasers Opt. 2021;127(2):1–9.
[23] Liu J, Tong Z, Zhang W, et al. Switchable and tunable multi-wavelength erbium-doped random distributed feedback fiber laser based on a compound filter. Opt. 2021;241:167015.
[24] Churkin DV, Babin SA, El-Taher AE, et al. Raman fiber lasers with a random distributed feedback based on Rayleigh scattering. Phys Rev A. 2010;82(3):10334–10338.
[25] Mahdi MA, Al-Mansoori MH, Premaratne M. Enhancement of multiwavelength generation in the L-band by using a novel brillouin-erbium fiber laser with a passive EDF booster section. Opt Express. 2007;15(18):11570–11575.